THE JOURNAL OF PHYSICAL CHEMISTRY B

 VOLUME 108, NUMBER 3, JANUARY 22, 2004

LETTERS

Photocatalytic Water Splitting into H_2 and O_2 over R_3TaO_7 and R_3NbO_7 (R = Y, Yb, Gd, La): Effect of Crystal Structure on Photocatalytic Activity

Ryu Abe,[†] Masanobu Higashi,[‡] Zhigang Zou,[†] Kazuhiro Sayama,[†] Yoshimoto Abe,[‡] and Hironori Arakawa*,[†]

Photoreaction Control Research Center (PCRC), National Institute of Advanced Industrial Science and Technology (AIST), 1-1-1 Higashi, Tsukuba, Ibaraki 305-8565, Japan, and Faculty of Science and Technology, Tokyo University of Science, Yamazaki 2641, Noda, Chiba 278-8514, Japan

Received: August 5, 2003; In Final Form: November 20, 2003

The photocatalytic activities of R_3TaO_7 and R_3NbO_7 (R = rare earth—Y, Yb, Gd, or La) were strongly dependent on the crystal structure. Photocatalytic splitting of pure water into H_2 and O_2 proceeded over NiO_x-loaded La_3TaO_7 and La_3NbO_7 photocatalysts with weberite-orthorhombic structure, while only a small amount of H_2 was evolved over other photocatalysts with cubic structure. In the case of the La_3TaO_7 and La_3NbO_7 photocatalyst, the phase transition from cubic into orthorhombic was observed at 1000−1050 °C, and the photocatalytic activity was drastically increased by phase transition from cubic into orthorhombic.

1. Introduction

Photocatalytic splitting of water into H_2 and O_2 using oxide semiconductor powder has received much attention for the potential application to direct production of H_2 for clean energy. Since the report of Fujishima and Honda on water splitting using TiO_2 photoelectrode,[1] numerous attempts have been made on the development of new semiconductor photocatalysts for efficient water splitting.[2−9] When semiconductor photocatalysts are used for water splitting, it is thermodynamically indispensable that the conduction band level should be more negative than the reduction potential of H_2O to form H_2 and the valence band should be more positive than the oxidation potential of H_2O to form O_2. However, it is rare that the splitting of pure water into H_2 and O_2 proceeds even if the semiconductor fulfills the above requirements of band structure. Not only charge generation but also following separation and migration of the charge are indispensable for water splitting to proceed. Although the efficiency of the charge separation and migration are certainly associated with the electronic and structural property of the semiconductor material, little attention has so far been given to the point.

To investigate the effect of crystal structure of semiconductor materials on the photocatalytic activity, we have chosen R_3TaO_7 and R_3NbO_7 (R = rare earth) systems as photocatalyst for water splitting. It has been reported that the crystal structure of R_3TaO_7 is more distorted for larger ionic radius of the R^{3+} ion, changing from fluorite-type cubic structure to pyrochlore-type cubic structure, then finally to weberite-type orthorhombic structure.[10,11] We found that the La_3TaO_7 and La_3NbO_7 photocatalysts with distorted orthorhombic structure exhibited higher activity than other photocatalysts with symmetric cubic structures.

2. Experimental Section

The powder samples of the R_3TaO_7 and R_3NbO_7 (R = rare earth) were prepared by a polymerized complex (PC) technique;

* Corresponding author. Fax: +81-29-856-3445. E-mail: h.arakawa@aist.go.jp.
[†] National Institute of Advanced Industrial Science and Technology (AIST).
[‡] Tokyo University of Science.

10.1021/jp036300v CCC: $27.50
Published on Web 12/24/2003

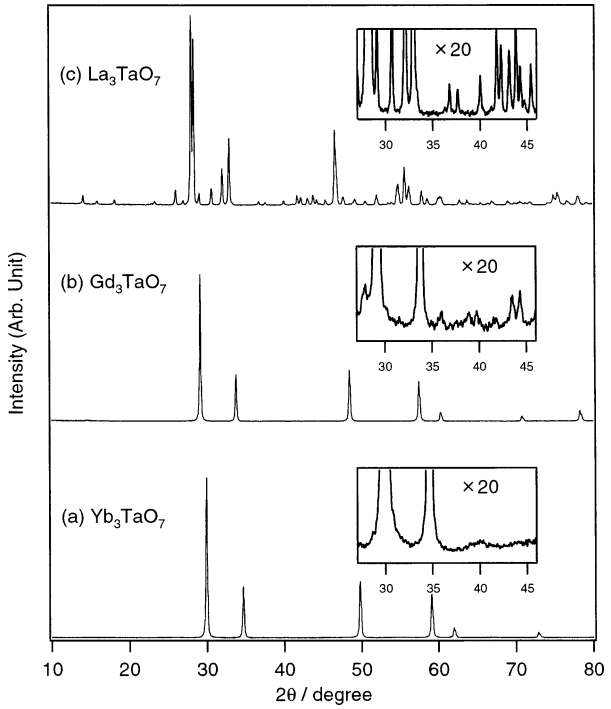

Figure 1. X-ray diffraction patterns of (a) Yb_3TaO_7, (b) Gd_3TaO_7, and (c) La_3TaO_7 prepared by the polymerized complex technique following the calcination at 1350 °C for 4 h.

the preparation procedure was basically followed with the report on Y_3NbO_7 by Kakihana et al.[12] Methanol (ca. 25 mL) was used as a solvent to dissolve 0.01 mol of $TaCl_5$ or $NbCl_5$. A large excess of citric acid (CA, 0.3 mol) was added into the methanol solution of $TaCl_5$ or $NbCl_5$ with continuous stirring to produce metal−CA complex. After complete dissolution of CA with methanol solution is achieved, 0.03 mol of $R(NO_3)_3 \cdot nH_2O$ (R = Y, Yb, Gd, La) was added, and the mixture was magnetically stirred for 1 h to produce a transparent solution of metal−CA complex. Subsequently, 0.4 mol of ethylene glycol (EG) was added to this solution. The clear solution thus prepared was heated at ∼130 °C to remove most of the methanol and subsequently to accelerate esterification reactions between CA and EG. On continued heating at ca. 130 °C, the solution became highly viscous with a change in color from colorless to deep brown, and finally it gelled into a transparent blown glassy resin. Charring the resin was carried out in an electric furnace for 2 h at 350 °C. The resulting black solid mass was ground into a powder, and then the powder precursor was calcined on an Al_2O_3 plate at 900−1350 °C for 4 h in static air, followed by natural (furnace) cooling to room temperature. The synthesized materials were confirmed by powder X-ray diffraction (MAC science, MX Labo). The surface area was determined by BET surface area measurement (Shimadzu, Gemini2360). Diffuse reflectance spectrum was measured by UV−vis spectrometry (JASCO, V-570) to estimate the band gap of photocatalyst.

NiO_x cocatalyst was loaded on the photocatalyst powder to promote H_2 production.[9] The photocatalyst powder prepared by the PC technique was immersed into an aqueous solution containing the required amount of $Ni(NO_3)_2$. The solution was then evaporated to the dry solid using a water bath, followed by heating in air at ca. 300 °C for 20 min. The NiO supported photocatalyst was then reduced by H_2 stream at 500 °C for 2 h and subsequent oxidation at 200 °C for 1 h in order to get NiO_x supported photocatalyst.

The photocatalytic reaction was examined using a gas closed circulation system. The photocatalyst powder (0.5 g) was dispersed in distilled water (400 mL) by a magnetic stirrer in an inner-irradiation reaction cell. The light source (400 W high-pressure mercury lamp, Riko Kagaku Japan) was covered with a water jacket (quartz glass; cutoff $\lambda < 200$ nm) to keep the reactor temperature constant at 20 °C by cooling water. The gases evolved were analyzed by on-line gas chromatography (TCD, molecular sieve 5A) connected with the circulation system.

TABLE 1: Water Splitting Activities and Crystal Structures of Prepared Photocatalysts

photocatalyst[a]	type of structure	rates of gas evolution (μmol h^{-1})[b] H_2	O_2	surface area (m^2 g^{-1})	band gap (eV)
Y_3TaO_7	fluorite-cubic	*c*	0	2.7	4.5
Yb_3TaO_7	fluorite-cubic	1	0	1.6	4.3
Gd_3TaO_7	pyrochlore-cubic	2.3	0	2.3	4.7
La_3TaO_7	weberite-orthorhombic	79	35	1.2	4.6
Y_3NbO_7	fluorite-cubic	*c*	0	2.1	3.9
Yb_3NbO_7	fluorite-cubic	2.1	0	1.2	3.8
Gd_3NbO_7	pyrochlore-cubic	0.4	0	3.0	3.9
La_3NbO_7	weberite-orthorhombic	7.0	3.0	1.3	3.9

[a] NiO loaded: 1 wt %. [b] Catalyst = 0.5 g; distilled water = 400 ml; light source = 400 W high-pressure mercury lamp; reaction cell = inner irradiation cell made of quartz. [c] Trace.

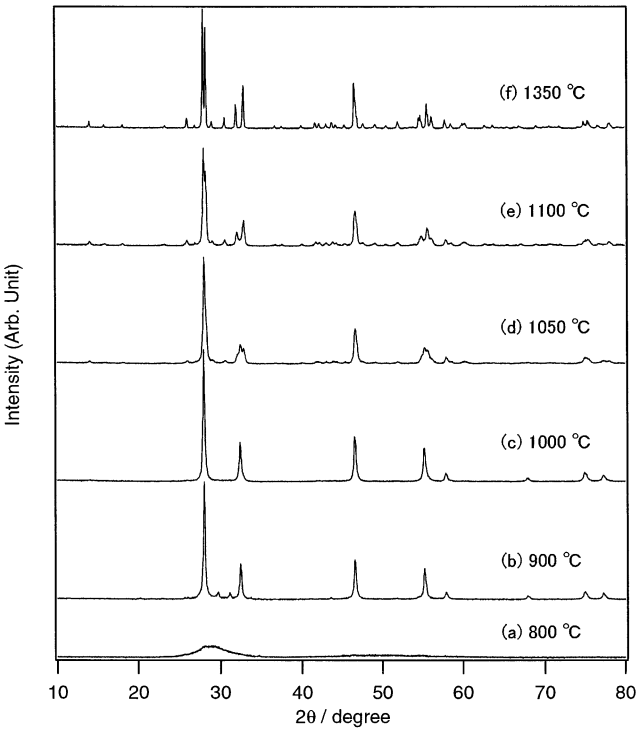

Figure 2. X-ray diffraction patterns of La_3TaO_7 samples prepared by the polymerized complex technique following the calcination in air at (a) 800, (b) 900, (c) 1000, (d) 1050, (e) 1100, and (f) 1350 °C for 4 h.

3. Results and Discussion

Figure 1 shows the X-ray diffraction (XRD) patterns of R_3TaO_7 samples (R = Yb, Gd, La) prepared by the PC technique following calcination at 1350 °C for 4 h. The XRD pattern of Y_3TaO_7 is not shown in Figure 1, because it was quite similar to that of Yb_3TaO_7. The XRD patterns of Y_3TaO_7 and Yb_3TaO_7, which include the small R^{3+} ions, Y^{3+} (0.88 Å) and Yb^{3+} (0.86 Å), were typical for a cubic fluorite structure.[8−10] In the diffraction patterns of Gd_3TaO_7 and La_3TaO_7 including the large R^{3+} ions, Gd^{3+} (0.94 Å) and La^{3+} (1.06 Å), several superlattice

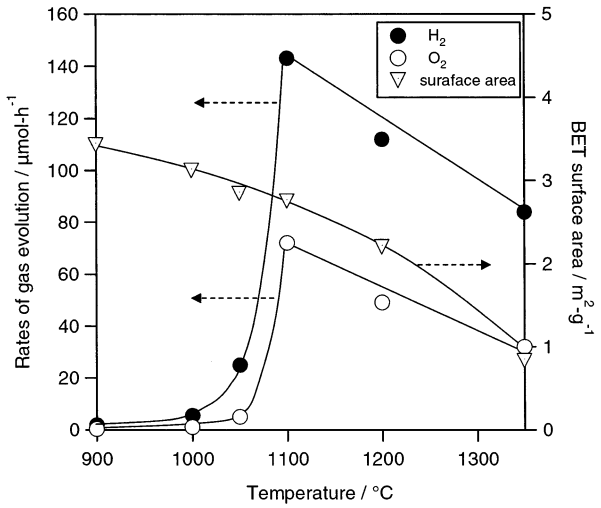

Figure 3. The rates of gas evolution (H_2, ●; O_2, ○) and the specific surface area (▽) of 1 wt % NiO−La_3TaO_7 samples as a function of calcination temperature.

lines appeared; the diffraction peaks of fundamental lines were apparently split. They were indicative of a cubic pyrochlore (Gd_3TaO_7) and an orthorhombic weberite structure (La_3TaO_7).[10,11] These XRD patterns of the samples prepared by the PC technique were identical to those of the samples prepared by solid-state reactions at 1700 °C for 4 h or at 1350 °C for 96 h, which were reported by Yokogawa et al.[10,11] Similar XRD patterns as those for R_3TaO_7 were observed for R_3NbO_7 samples, except for the slight difference in the lattice parameters.

The photocatalytic activities of NiO_x (1 wt %)-loaded R_3TaO_7 and R_3NbO_7 samples for the splitting of distilled water and the crystal structure of them are summarized in Table 1 (samples were prepared at 1350 °C). La_3TaO_7 and La_3NbO_7 with weberite-orthorhombic structure showed activities for H_2 and O_2 evolution from distilled water in the stoichiometric ratio (H_2:O_2 = 2:1) within an experimental error. Over the other photocatalysts with cubic structure, only a small amount of H_2 but no O_2 was evolved, and then the reaction was terminated in several hours. No structural change of the samples was observed in the XRD patterns after the reaction.

The band gaps of R_3TaO_7 and R_3NbO_7 samples estimated from the onset of UV−vis absorption spectra were 4.3−4.6 and 3.8−3.9 eV, respectively (see Table 1). This indicates that the effect of R^{3+} ion on the band structure was not so significant in these materials. The BET surface areas of these materials prepared at 1350 °C were similar in the range of 1.2−3.0 m^2/g (see Table 1). It was therefore speculated that the difference of the crystal structure significantly affected the photocatalytic activity of these materials.

To confirm the effect of crystal structure on photocatalytic activity, we carried out detailed investigation on the La_3TaO_7 and La_3NbO_7 photocatalysts. During the preparation of the La_3TaO_7 and La_3NbO_7 photocatalysts by the PC method, we found that a phase transition from cubic to orthorhombic occurs at around 1050 and 1000 °C, respectively. As shown in Figure 2, the XRD patterns of some La_3TaO_7 samples prepared below 1000 °C indicate typical cubic structure like Gd_3TaO_7, while those above 1100 °C indicate orthorhombic weberite structure. To our best knowledge, the synthesis of La_3TaO_7 and La_3NbO_7 with cubic phase has not been reported by the preparation method of traditional solid-state reaction. The low temperature synthesis by the PC technique certainly enabled the generation of the cubic phase.

The rate of H_2 and O_2 gas evolution for the NiO_x−La_3TaO_7 samples are plotted as a function of the calcination temperature in Figure 3, wherein data for the specific surface area of each sample is also shown. The rates of gas evolution drastically increased with the increase of the temperature from 1000 to 1100 °C. During this temperature interval, the phase transition from cubic to orthorhombic phase has occurred. Then the rate of gas evolution has gradually decreased above 1100 °C. The decrease in gas evolution rates above 1100 °C is possibly due to the decrease in the surface area. Similar tendency was observed for the NiO_x−La_3NbO_7 photocatalysts. Figure 4a shows the time course of gas evolution over NiO_x (1 wt %)-loaded La_3TaO_7 photocatalysts prepared at 1000 °C (cubic) and 1100 °C (orthorhombic), respectively. The La_3TaO_7 with orthorhombic structure exhibited much higher activity (H_2 = 164 μmol/h, O_2 = 82 μmol/h) than that of the La_3TaO_7 with cubic structure (H_2 = 4 μmol/h, O_2 = 1 μmol/h). The induction period in the first hour might be attributable to the time for activation of surface of the photocatalyst or for dispersion of the photocatalyst powder in water. The orthorhombic La_3NbO_7 (prepared at 1100 °C) also exhibited much higher activity than that of the cubic one as shown in Figure 4b. These results clearly indicate that the crystal structure, rather than the constitute elements, affects the activity of these photocatalysts. The results in Table 1 and Figure 3 indicate that the R_3TaO_7 and R_3NbO_7 compounds with distorted orthorhombic structure exhibit higher

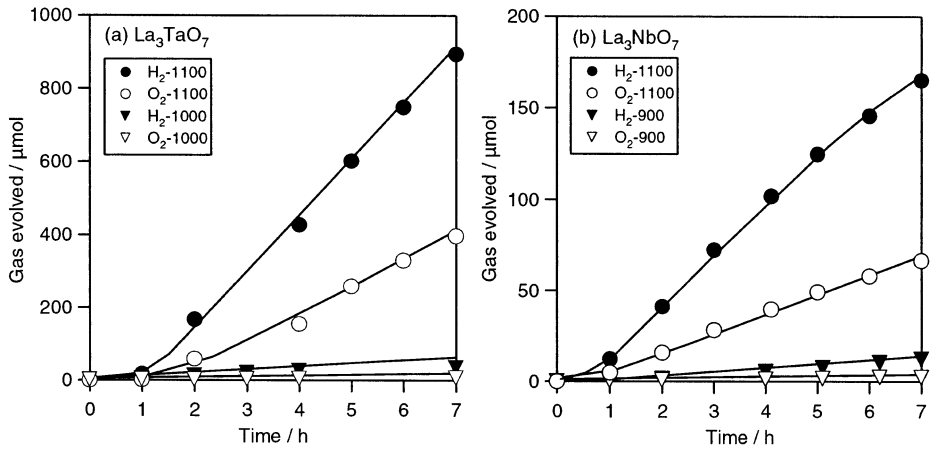

Figure 4. Reaction time courses of gas evolution from distilled water (400 mL) over 1 wt % NiO_x−La_3TaO_7 and 1 wt % NiO_x−La_3NbO_7 photocatalysts under UV light irradiation: (a) La_3TaO_7 photocatalyst prepared by calcination at 1000 °C (cubic; H_2, ▼; O_2, ▽) and at 1100 °C (orthorhombic; H_2, ●; O_2, ○); (b) La_3NbO_7 photocatalyst prepared by calcination at 900 °C (cubic; H_2, ▼; O_2, ▽) and 1100 °C (orthorhombic; H_2, ●; O_2, ○).

photocatalytic activity than those with symmetric cubic structure. The dipole moment generated by the distortion in crystal structure might improve the separation of electron−hole pairs in the semiconductor photocatalyst. Alternatively, the phase transition might bring the change in resistance of the materials, and this influences the mobility of charge and the photocatalytic activity consequentially.

Conclusion

We prepared the series of R_3TaO_7 and R_3NbO_7 (R = rare earth−Y, Yb, Gd, or La) by the polymerized complex (PC) technique and investigated their photocatalytic activity for splitting of pure water into H_2 and O_2. The crystal structures of R_3TaO_7 and R_3NbO_7 changed with increasing ionic radius of the R^{3+} ion from fluorite-type cubic structure to pyrochlore-type cubic structure and finally to weberite-type orthorhombic structure. The water splitting into H_2 and O_2 in a stoichiometric ratio proceeded over NiO_x-loaded La_3TaO_7 and La_3NbO_7 photocatalysts with distorted orthorhombic structure. In both cases of La_3TaO_7 and La3NbO7, the phase transition from cubic into orthorhombic phase was observed at around 1000−1050 °C, and the photocatalytic activity was drastically increased by the phase transition from cubic to orthorhombic phase. These results indicate the significant influence of crystal structure on the photocatalytic activity of the oxide semiconductor materials.

Acknowledgment. This work was supported by the Fund for Young Researchers, Ministry of Education, Culture, Sport, Science and Technology.

References and Notes

(1) Fujishima, A.; Honda, K. *Nature* **1972**, *238*, 37.
(2) Lehn, J. M.; Sauvage, J P.; Ziessel, R. *Nouv. J. Chim.* **1980**, *4*, 623.
(3) Domen, K.; Kudo, A.; Onishi, T. *J. Catal.* **1986**, *102*, 92.
(4) Kudo, A.; Tanaka, A.; Domen, K.; Maruya, K.; Aika, K.; Onishi, T. *J. Catal.* **1988**, *111*, 67.
(5) Inoue, Y.; Kubokawa, K.; Sato, K. *J. Phys. Chem.* **1991**, *95*, 4059.
(6) Inoue, Y.; Kohno, M.; Kaneko, T.; Ogura, S.; Sato, K. *J. Chem. Soc., Faraday Trans.* **1998**, *94*, 89.
(7) Machida, M.; Yabunaka, J.; Kijima, T. *Chem. Mater.* **2000**, *12*, 812.
(8) Hwang, D. W.; Kim, H. G.; Kim, J.; Cha, K. Y.; Kim, Y. G.; Lee, J. S. *J. Catal.* **2000**, *193*, 40.
(9) Kato, H.; Asakura, K.; Kudo, A. *J. Am. Chem. Soc.* **2003**, *125*, 3082.
(10) Yokogawa, Y.; Yoshimura, M.; Somiya, S. *Mater. Res. Bull.* **1987**, *22*, 1449.
(11) Yokogawa, Y.; Yoshimura, M.; Somiya, S. *Solid State Ionics* **1988**, *28*, 1250.
(12) Okubo, T.; Kakihana, M. *J. Alloys Compd.* **1997**, *256*, 151.